

## Effects of $\gamma$ -Fe<sub>2</sub>O<sub>3</sub> on the transport critical current density of (Bi<sub>1.6</sub>Pb<sub>0.4</sub>)Sr<sub>2</sub>Ca<sub>2</sub>Cu<sub>3</sub>O<sub>10</sub> superconductors

S. Y. YAHYA\*, M. H. JUMALI, C. H. LEE, R. ABD-SHUKOR‡

School of Applied Physics, Universiti Kebangsaan Malaysia, 43600, Bangi, Selangor, Malaysia

E-mail: ras@pkrisc.cc.ukm.my

The inclusion of submicron or nano-sized particles in materials may have a drastic effect on their physical properties. Studies on the transport critical current density in the copper oxide based high temperature superconductors (HTSC) is interesting from the basic understanding point of view as well as for the advancement of their application.

One of the widely studied HTSC is the Bi-system of copper oxide-based high temperature superconductor. A number of theoretical and experimental results have been reported on the transport current in this system. This includes introduction of submicron and nano-size columnar defects as flux pinning center [1, 2]. Ultra-fine defects may be able to minimize the pinning interaction of the flux line without suppressing the superconducting volume. The introduction of magnetic nanorod and submicron dots has also been proposed to achieve a frozen flux superconductor [3–5]. In addition some experimental and theoretical studies have shown the positive effect of superconducting nanoparticles on the transition temperature of these high  $T_c$  materials [6, 7].

Flux line network and magnetic texture can interact effectively if their characteristic scales have the same order of magnitude. The characteristic scales for flux line network is the coherence length  $\xi$ , which varies in range of 1 to 100 nm. Another characteristic length is the penetration depth  $\lambda$ , which is in the range of 60 to 1000 nm. In a magnetic system with the characteristic length  $\xi < L < \lambda$ , where  $L$  is the size of the pinning center, a strong interaction between flux line network and magnetic subsystem can be expected [4]. It is interesting to investigate further the possibility of a frozen flux superconductor in such a superconductor-magnet hybrid system.

The addition of nano-size MgO was found to increase the critical current when the maximum heat treatment temperature was 910 °C [8]. However, no significant enhancement of  $J_c$  was evidenced after nano-metric SnO<sub>2</sub> powder was added into YBCO [9]. The incorporation of ultrafine impurities with submicron diameter has some positive effect on the critical current in the YBCO superconductors [10].

In this work magnetic nano-particle, maghemite ( $\gamma$ -Fe<sub>2</sub>O<sub>3</sub>) of about 50 nm in radius with rod-like shape was used to act as pinning centers in bulk

(Bi<sub>1.6</sub>Pb<sub>0.4</sub>)Sr<sub>2</sub>Ca<sub>2</sub>Cu<sub>3</sub>O<sub>10</sub> (Bi-2223) superconductor. The transition temperature, transport critical current density, microstructure, and X-ray diffraction pattern are reported.

Samples with nominal composition (Bi<sub>1.6</sub>Pb<sub>0.4</sub>)-Sr<sub>2</sub>Ca<sub>2</sub>Cu<sub>3</sub>O<sub>10</sub> were prepared from powders of Bi<sub>2</sub>O<sub>3</sub>, PbO, SrO, CaO and CuO of at least 99.9% purity. The powders were calcined at 800 °C for 24 hrs. Further calcination was done at 830 °C for 24 hrs after re-grinding. The powders were then pressed into pellets of approximately 1.3 cm diameter and 2 mm thickness and heated for 150 hrs at 850 °C. After the sintering process  $\gamma$ -Fe<sub>2</sub>O<sub>3</sub> was added to the composition with (Bi<sub>1.6</sub>Pb<sub>0.4</sub>)Sr<sub>2</sub>Ca<sub>2</sub>Cu<sub>3</sub>O<sub>10</sub>-( $\gamma$ -Fe<sub>2</sub>O<sub>3</sub>)<sub>x</sub> with  $x = 0.00, 0.01, 0.02, 0.03, 0.04, 0.05$ , and 0.1. The powders were mixed in an agate mortar, pressed into pellets, and calcined at 840 °C for 50 hrs.

The electrical resistance was measured using the standard four-point probe method with silver paints contact in conjunction with a CTI Cryogenic Closed Cycle refrigerator Model 21. The pellets were cut into a bar shape with an approximate cross sectional dimension of 2 mm × 3 mm. The transport critical current,  $I_c$  was determined from the I-V characteristic at 77 K using the 1  $\mu$ V/cm criterion. The transport critical current density  $J_c$  was calculated by dividing the critical current  $I_c$  of the bar sample with the corresponding cross sectional area. A Philips XL-30 scanning electron microscope was used to observe the microstructure of the bulk superconductor samples while observation for  $\gamma$ -Fe<sub>2</sub>O<sub>3</sub> was done with LEO 1450VP scanning electron microscope. A Bruker D8 Advance diffractometer with Cu K $\alpha$  radiation was used to determine the X-ray diffraction pattern.

Fig. 1 shows the randomly oriented rod-like shape  $\gamma$ -Fe<sub>2</sub>O<sub>3</sub> of approximately 100 nm long and 50 nm radius. In order to make a comparison between (Bi<sub>1.6</sub>Pb<sub>0.4</sub>)Sr<sub>2</sub>Ca<sub>2</sub>Cu<sub>3</sub>O<sub>10</sub> with and without  $\gamma$ -Fe<sub>2</sub>O<sub>3</sub>, a (Bi<sub>1.6</sub>Pb<sub>0.4</sub>)Sr<sub>2</sub>Ca<sub>2</sub>Cu<sub>3</sub>O<sub>10</sub> superconductor without  $\gamma$ -Fe<sub>2</sub>O<sub>3</sub> was prepared as a reference sample. The micrograph of a fractured surface of the reference sample is shown in Fig. 2. The figure shows randomly oriented grains, implying the occurrence of a rather large number of weak links. The sample has a critical current density  $J_c$  of about 600 A/cm<sup>2</sup>. Fig. 3 shows the fractured surface of the  $x = 0.01$  sample. It clearly shows

\*Permanent address: Universiti Teknologi Mara, Cawangan Pahang, 26400, Bandar Jengka, Pahang, Malaysia.

‡Author to whom all correspondence should be addressed.

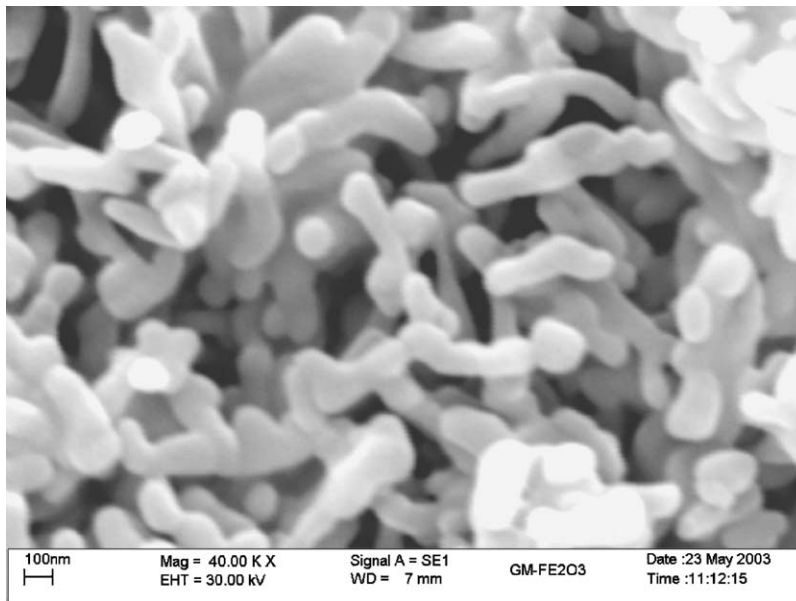


Figure 1 Micrograph of rod-like structure of  $\gamma$ -Fe<sub>2</sub>O<sub>3</sub>.

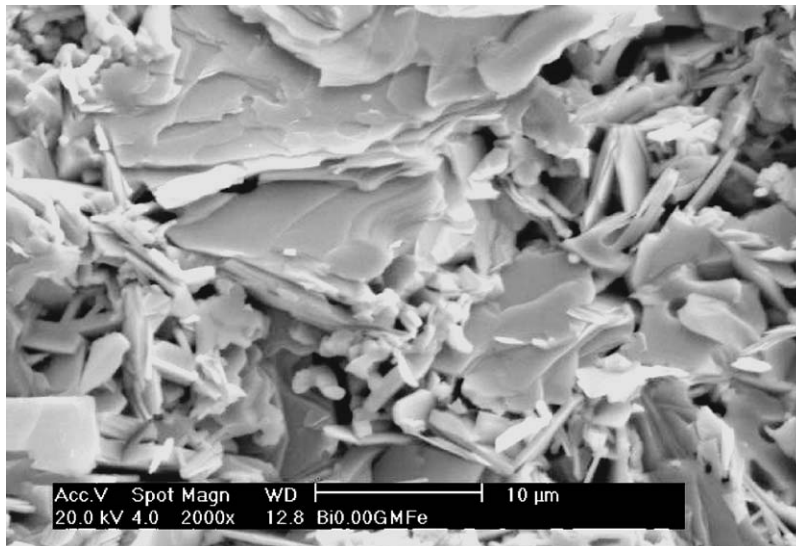


Figure 2 Micrograph of  $(\text{Bi}_{1.6}\text{Pb}_{0.4})\text{Sr}_2\text{Ca}_2\text{Cu}_3\text{O}_{10}$  without  $(\gamma\text{-Fe}_2\text{O}_3)_x$ .

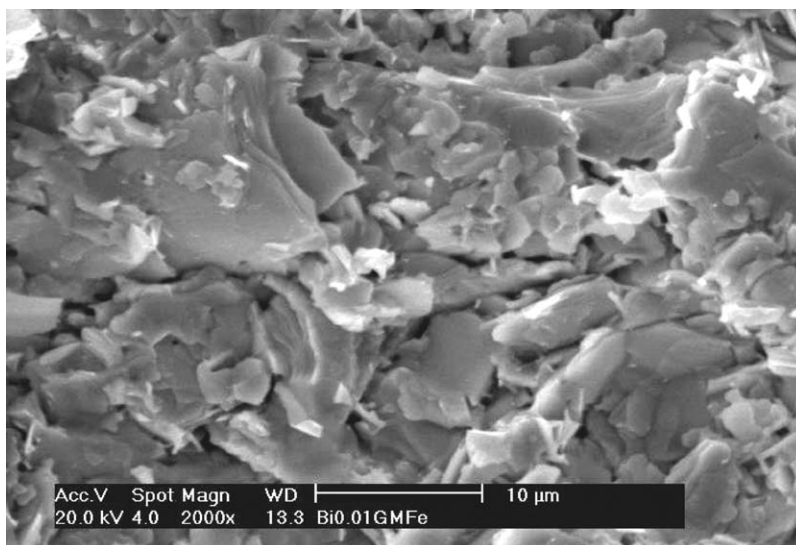


Figure 3 Micrograph of  $(\text{Bi}_{1.6}\text{Pb}_{0.4})\text{Sr}_2\text{Ca}_2\text{Cu}_3\text{O}_{10}-(\gamma\text{-Fe}_2\text{O}_3)_x$  with  $x = 0.01$ .

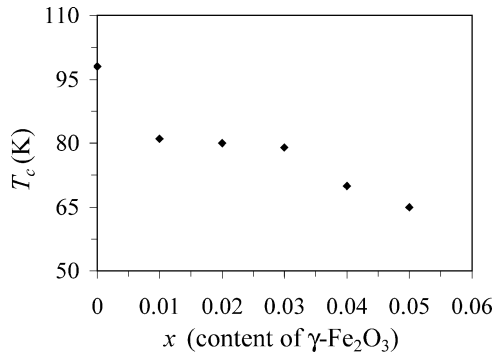


Figure 4  $T_c$  vs.  $x$ , of  $(\text{Bi}_{1.6}\text{Pb}_{0.4})\text{Sr}_2\text{Ca}_2\text{Cu}_3\text{O}_{10}-(\gamma\text{-Fe}_2\text{O}_3)_x$ .

the stacking up of layers which contributed to a higher  $J_c \approx 1100 \text{ A/cm}^2$ .

The effect of  $\gamma\text{-Fe}_2\text{O}_3$  on the  $T_c$  for  $(\text{Bi}_{1.6}\text{Pb}_{0.4})\text{Sr}_2\text{Ca}_2\text{Cu}_3\text{O}_{10}-(\gamma\text{-Fe}_2\text{O}_3)_x$  samples with  $x = 0.00$  to  $0.05$  are shown in Fig. 4.  $T_c$  is defined as the temperature at which the resistance of the sample reached zero. For non-substituted sample, the  $T_c$  is around 98 K. At  $x = 0.01$ ,  $T_c$  is suppressed to approximately 81 K. Further addition of  $\gamma\text{-Fe}_2\text{O}_3$  reduces  $T_c$  to 80 K ( $x = 0.02$ ), 79 K ( $x = 0.03$ ) and 65 K ( $x = 0.05$ ).

Fig. 5 shows the X-ray diffraction patterns of  $(\text{Bi}_{1.6}\text{Pb}_{0.4})\text{Sr}_2\text{Ca}_2\text{Cu}_3\text{O}_{10}-(\gamma\text{-Fe}_2\text{O}_3)_x$  with  $x = 0.00, 0.01, 0.03$ , and  $0.05$ . The main peaks in the XRD patterns can be identified as  $(00l)$  peaks of Bi-2223 and

TABLE I Variation of volume fraction of Bi-2223 and Bi-2212 phase with addition of  $\gamma\text{-Fe}_2\text{O}_3$

$x$	$V_{2223}(\%)$	$V_{2212}(\%)$
0.00	62	38
0.01	57	43
0.03	39	61
0.05	40	60

Bi-2212 phases while the peaks of the Bi-2201 are not observed. Some non-superconducting phases such as  $\text{Ca}_2\text{CuO}_3$  can also be detected. The volume fraction of the 2223 and 2212 phase were determined from the intensity ( $I$ ) of the XRD pattern using the formula by  $(I_{H(0010)})/(I_{H(0010)} + I_{L(008)})$ .  $H$  and  $L$  stand for the high  $T_c$  phase (Bi-2223) and low  $T_c$  phase (Bi-2212), respectively and shown in Table I. The volume fraction of Bi-2223 is found to decrease with increasing  $\gamma\text{-Fe}_2\text{O}_3$  concentration, indicating that the addition of  $\gamma\text{-Fe}_2\text{O}_3$  does not favor Bi-2223 conversion from Bi-2212 phase. This effect may be due to the fact that  $\gamma\text{-Fe}_2\text{O}_3$  retards the insertion process of Ca-Cu-O layer into Bi-2212. Intercalation mechanism suggests that Bi-2223 phase is formed from layer by layer intercalation of Ca-Cu-O bilayers into the existing Bi-2212. However the intercalation would be impeded by  $\gamma\text{-Fe}_2\text{O}_3$  when the moving Ca-Cu-O bilayers meet  $\gamma\text{-Fe}_2\text{O}_3$  embedded in Bi-2212

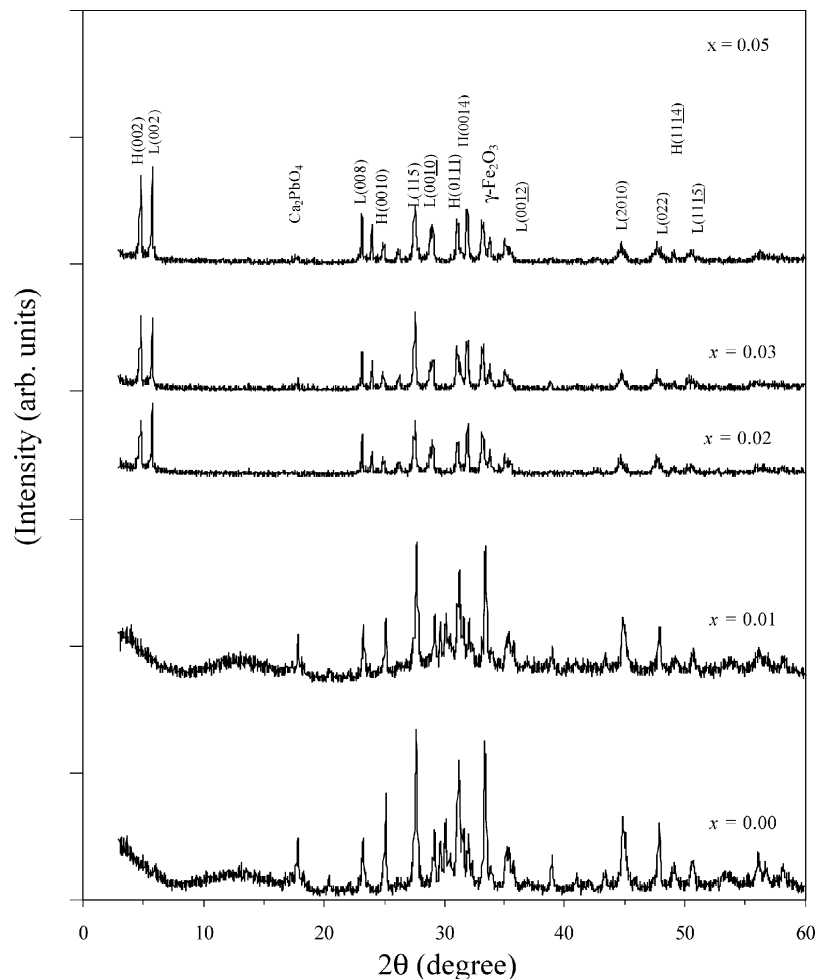


Figure 5 X-ray diffraction patterns for  $(\text{Bi}_{1.6}\text{Pb}_{0.4})\text{Sr}_2\text{Ca}_2\text{Cu}_3\text{O}_{10}-(\gamma\text{-Fe}_2\text{O}_3)_x$ .

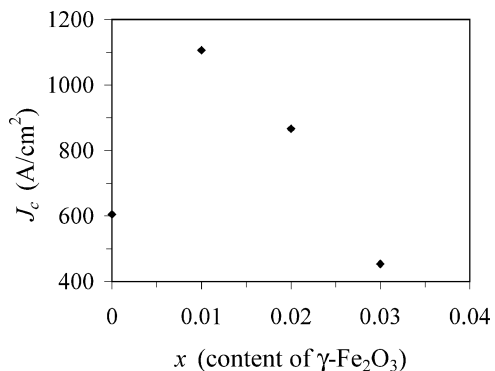


Figure 6  $J_c$  vs.  $x$  of  $(\text{Bi}_{1.6}\text{Pb}_{0.4})\text{Sr}_2\text{Ca}_2\text{Cu}_3\text{O}_{10}-(\gamma\text{-Fe}_2\text{O}_3)_x$  at 77 K.

matrix and thus the conversion to Bi-2223 is retarded as observed in other materials [11].

$J_c$  at 77 K for  $x = 0.00, 0.01, 0.02,$  and  $0.03$  are shown in Fig. 6. Maximum  $J_c \approx 1100 \text{ A/cm}^2$  was achieved in the  $x = 0.01$  sample followed by a decrease with higher content of  $\gamma\text{-Fe}_2\text{O}_3$ . It is well known that the  $J_c$  values depend on the volume fraction of the Bi-2223 phase.

In conclusion, the effect of nano-sized  $\gamma\text{-Fe}_2\text{O}_3$  on the transport properties of  $(\text{Bi}_{1.6}\text{Pb}_{0.4})\text{Sr}_2\text{Ca}_2\text{Cu}_3\text{O}_{10}-(\gamma\text{-Fe}_2\text{O}_3)_x$  for  $x = 0-0.1$  is reported. The addition of  $\gamma\text{-Fe}_2\text{O}_3$  is found to enhance the transport critical current density measured at 77 K of the  $x = 0.01$  sample. Although the addition of a small amount ( $x = 0.01$ ) of  $\gamma\text{-Fe}_2\text{O}_3$  decreased the percentage of 2223 phase, the magnetic nano particles can improve the flux pinning properties of the superconductor, which indicates the possibility of a frozen flux in such a hybrid system. It would be interesting to see if this method of nano-sized  $\gamma\text{-Fe}_2\text{O}_3$  inclusion can be employed to increase

the transport critical current density of HTSC tapes and thin films.

### Acknowledgment

This work has been supported by the Ministry of Science, Technology, and Innovation of Malaysia under IRPA grant no. 09-02-02-0072-EA199.

### References

1. Y. ZHU, Z. X. CAI, R. C. BUDHARI, M. SUANAGA and D. O. WELCH, *Phys. Rev. B* **48** (1993) 6436.
2. P. YANG and C. M. LIEBER, *Science* **273** (1996) 1836.
3. J. I. MARTIN, M. VELEZ, J. NOGUES and I. K. SCHULLER, *Phys. Rev. Lett.* **79** (1997) 1927.
4. I. F. LYUKSYUTOV and D. G. NAUGLE, *Modern Phys. Lett. B* (1999) 491.
5. I. F. LYUKSYUTOV, D. G. NAUGLE and V. POKROVSKY, in Proceedings of SPIE, edited by D. Pavuna and I. Bozovic (Superconducting and Related Oxides, Physics of Nano-engineering IV, 2000) Vol. 4058, p. 376.
6. V. A. IVANOV, V. R. MISKO, V. M. FOMIN and J. T. DEVREESE, *Solid State Comm.* **125** (2003) 439.
7. D. C. RALPH, C. T. BLACK and M. THINKHAM, *Phys. Rev. Lett.* **78** (1997) 4087.
8. K. CHRISTOVA, A. MANOV, J. NYHUS, U. THISTED, O. HERSTAD, S. E. FOSS, K. N. HAUGEN and K. FOSSHEIM, *J. Alloys Comp.* **340** (2002) 1.
9. Z. H. HE, T. HABISRUETHER, G. BRUCHLOS, D. LITZKENDORF and W. GAWALEK, *Physica C* **356** (2001) 277.
10. I. ZHOU, S. K. CHEN, K. G. WANG, X. Z. WU, P. X. ZHANG and Y. FENG, *ibid.* **362** (2001) 99.
11. B. ZHAO, X. WAN, W. SONG, Y. SUN and J. DU, *ibid.* **337** (2000) 138.

Received 21 April

and accepted 28 May 2004